SARSense: Analyzing air- and space-borne C- and L-band SAR backscattering signals to changes in soil and plant parameters of crops

David Mengen[1*], Carsten Montzka[1], Thomas Jagdhuber[2,3], Anke Fluhrer[2,3], Cosimo Brogi[1], Stephani Baum[4], Dirk Schüttemeyer[5], Bagher Bayat[1], Heye Bogena[1], Alex Coccia[6], Gerard Masalias[6], Verena Trinkel[4], Jannis Jakobi[1], Francois Jonard[1,7], Yueling Ma[1], Francesco Mattia[8], Davide Palmisano[8], Uwe Rascher[4], Giuseppe Satalino[8], Maike Schumacher[9], Christian Koyama[10], Marius Schmidt[1], and Harry Vereecken[1]

[1] Forschungszentrum Jülich, Institute of Bio-and Geosciences: Agrosphere (IBG-3), Jülich, Germany
[2] German Aerospace Center, Microwaves and Radar Institute, Wessling, Germany
[3] University of Augsburg, Institute of Geography, Augsburg, Germany
[4] Forschungszentrum Jülich, Institute of Bio- and Geosciences: Plant Sciences (IBG-2), Jülich, Germany
[5] European Space Agency, Mission Science Division, Noordwijk, The Netherlands
[6] Metasensing BV, Noordwijk, The Netherlands
[7] Universite catholique de Louvain, Earth and Life Institute, Louvain-la-Neuve, Belgium
[8] Consiglio Nazionale delle Ricerche (CNR), Institute for Electromagnetic Sensing of the Environment (IREA), Bari, Italy
[9] Aalborg University, Geodesy and Surveying, Aalborg, Denmark
[10] Tokyo Denki University, School of Science and Engineering, Tokyo, Japan
* Correspondence: d.mengen@fz-juelich.de

IGARSS 2021 - 2021 IEEE International Geoscience and Remote Sensing Symposium | 978-1-6654-0369-6/21/$31.00 ©2021 IEEE | DOI: 10.1109/IGARSS47720.2021.9553399

ABSTRACT

The upcoming launch of the L-band Synthetic Aperture Radar (SAR) satellite mission Radar Observing System for Europe L-band SAR (ROSE-L) will enable multi-frequency SAR observations when combined with existing C-band satellite missions (e.g., Sentinel-1). Due to the different penetration depths of the SAR signals, multi-frequency SAR offers great potential for field-scale agricultural monitoring and the estimation of soil and plant parameters. The SARSense campaign, conducted between June and August 2019 at the Selhausen agricultural test site near Jülich, Germany, has yielded a comprehensive dataset that includes both air- and space-borne C- and L-band SAR data, extensive in-situ field measurements of soil and plant parameters as well as unmanned aerial systems (UAS)-based multispectral and thermal infrared measurements and cosmic neutron sensing observations. The study provides both, an insight into the strengths and limitations of the acquired dataset as well as an analysis of the different behaviour of C- and L-band backscattering on changing soil moisture and plant parameters for taproot crops and cereals.

1. INTRODUCTION

The monitoring of soil moisture and vegetation parameters at both, global and local scales, is a key challenge, which can be addressed by modern Earth Observation satellites [1,2]. By using multi-frequency SAR acquisitions, the weather-independent observation of the Earth's surface during day and night is possible, as well as the different wavelengths of the SAR signals can accommodate to the change in vegetation parameters (structure & moisture) during the growing season [3]. In this regard, especially for heterogeneous agricultural sites with different crops, multi-frequency SAR observations have a high potential for the estimation of soil and vegetation parameters and their continuous monitoring in time and space. As the upcoming launch of the L-band ROSE-L satellite mission in 2028 and its integration into the existing (and future) C-band satellite mission Sentinel-1 A/B (C/D) will enable quasi multi-frequency SAR acquisitions, the SARSense campaign was conducted as a precursor to analyze both, the sensitivity of high-resolution C- and L-band backscattering signals to changes in key agricultural parameters (e.g., soil moisture, vegetation water content (VWC)) for different crops as well as the synergy effects of a spatially and temporally close/proximate acquisition.

2. STUDY AREA

The Selhausen test site, located in the Eastern part of the Rur catchment in Germany (50.865°N, 6.447°E), has an area of about 1 km² and consists of 56 individual agricultural fields, representing the diverse and small-scale cropping structure of the agricultural land cover of the Lower Rhine Embayment (figure 1). The test site is located in the tempered maritime climate zone, with a mean annual temperature of 10.2 °C and mean annual

precipitation of 741 mm. During the SARSense campaign, winter wheat, sugar beet, winter barley, potato, silage maize, winter rapeseed, cabbage, oat and rye were cultivated. The main types of soil that are prevalent are (gleyic) Luvisol and (gleyic) Cambisol, with a majorly silty loam texture [4]. The grain size in the uppermost 30 cm of soil is highly variable with 13% - 35% sand, 52% - 70% silt and 13% - 17% clay [5]. Recent studies revealed a historic river channel system on the test site by remotely sensing the Leaf Area Index (LAI) and crop modelling, leading to highly variable soil moisture contents and different crop development especially during dry conditions [6–8]. As the SARSense campaign was conducted during a severe drought, the observed soil moisture contents were low to very low, with a mean of 8 vol.% in June and 17 vol.% in August. Nevertheless, due to the historic river channels as well as regular irrigation by the farmers and specific field experiments, the variability in soil moisture was comparably high (0 vol.% to 48 vol.%).

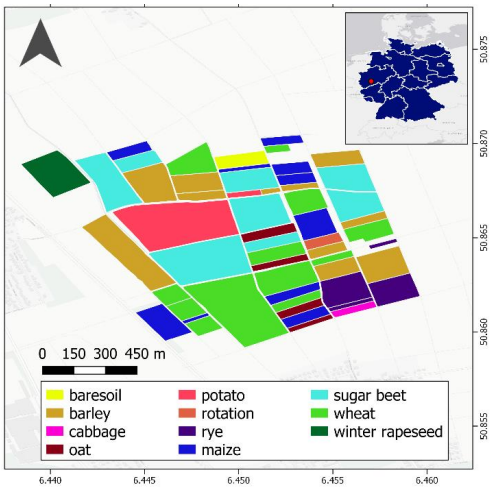

Figure 1 Map of the Selhausen test site and the individual crop types during the SARSense campaign period in 2019.

3. DATA

Fully polarized (HH, HV, VH, VV) airborne C- and L-band SAR acquisitions were recorded on the 19th, 21st, 25th and 27th of June as well as on the 8th and 9th of August 2019. For each day, the same three flight tracks were flown, two in ascending and one descending direction, resulting in an 20 % overlap of adjacent scenes. In addition, in-situ soil moisture and other soil parameters (e.g., temperature, bulk electrical conductivity, pore water electrical conductivity, dielectric permittivity) were sampled on the respective dates. Plant parameters (e.g., fresh/dry weight of leaves

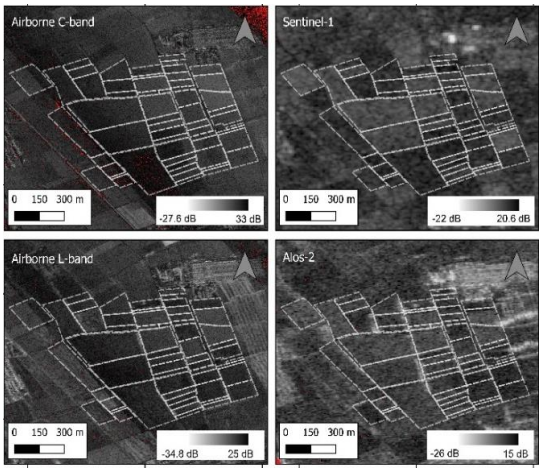

Figure 2 Comparison of air- and space-borne C- and L-band observations in decibel (dB) over the Selhausen test site for the 21st / 22nd of June2019; white polygons indicate fields boundaries.

and stems, LAI, plant height, leaf chlorophyll concentration), were sampled on the 25th of June and 7th of August 2019. Furthermore, 58 Sentinel-1 (VV and VH) and 6 ALOS-2 scenes (HH and HV) were acquired in the period from the 1st of June to 31st of August 2019 (figure 2). RGB orthomosaics for the whole study site were recorded on the 17th and 26th of June, the 3rd and 25th of July and 8th of August 2019 as well as multispectral and thermal infrared measurements on the 26th and 27th of June 2019. Cosmic-ray neutron sensing was performed on the 27th of June and 8th of August 2019, using a vehicle-based cosmic-ray rover. Due to involvement in various environmental monitoring programs (e.g., TERENO), additional data are routinely and continuously collected during the campaign period. Three climate stations and two eddy covariance stations, a groundwater well and four automated closed dynamic chambers for measuring soil CO_2 emissions are permanently installed on site as well as 18 lysimeters and two rhizotrone facilities.

4. TEMPORAL VARIATIONS OF AIR- AND SPACE-BORNE SAR DATA

Due to a misalignment of corner reflectors during the airborne SAR acquisitions, no absolute radiometric calibration could be achieved. The observations were instead calibrated among themselves, using the noise level of the first data take as a reference and calculating a relative noise level for the other observations to level out temporal variations. A Sentinel-1 scene was used for calculating global calibration factors, to minimize

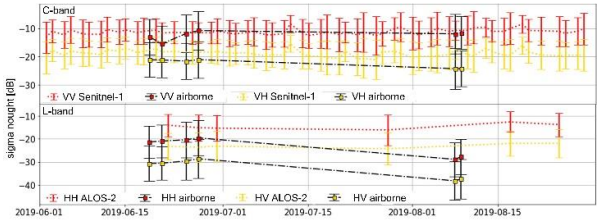

Figure 3 Time series of polarimetric backscattering signal of C- and L- band air- and space-borne data.

the offset between C- and L-band air- and space-borne backscattering signals.

Comparing the temporal behavior of the calculated mean values of the backscattering signal from airborne and space-borne SAR observations, the airborne data differ both in absolute values and in their temporal behavior from the space-borne data (figure 3). As this is likely due to the calibration process rather than caused by temporal changes in soil and plant parameters, the airborne data should be used for scene-based (spatial) analyses, while the space-borne data can be used also for comparing measurements from different dates.

5. RELATION OF BACKSCATTERING SIGNALS TO SOIL AND PLANT PARAMETERS

Analyzing the behaviour of C- and L-band backscattering signals to changes of soil and plant parameters, the study focused on soil moisture, VWC, plant height as well as the UAS-based Normalized Difference Red Edge Index (NDRE) for the crops sugar beet, potato, wheat and barley. In this regard, the mean backscattering signals within an 11-m radius around each measurement location were correlated to the corresponding parameter and evaluated using R^2 and RMSD from linear regression models. For analysing soil moisture, Sentinel-1 scenes from the 21st and 27th of June 2019 and ALOS-2 scenes from 22nd and 27th of June 2019 were correlated to in-situ measurements from 21st and 27th of June 2019. For the correlation between backscattering signal and VWC as well as plant height, Sentinel-1 scenes from the 26th of June and the 7th of August 2019 and ALOS-2 scenes from the 27th of June were used. For the scene-based, spatial analysis of the airborne data, the SAR observations from 27th of June 2019 were correlated to the corresponding NDRE values. In addition, due to the partial irrigation of the potato field F11 by the farmer during the airborne SAR acquisition on the 27th of June 2019, the effect of interception water on the backscattering signal was analysed.

For both C- and L-band, the lowest correlation can be observed between backscattering signal and soil moisture, with R^2 values below 0.35 (C-band) and 0.36 (L-band). At L-band, the highest correlations can be observed for wheat, while at C-band, the highest correlation can be observed for potato. Regarding VWC, higher correlations are present, with R^2 values of up to 0.65 at C-band and up to 0.64 at L-band. While the highest correlation in L-band can be observed for wheat and barley, C-band shows higher correlations for potato and sugar beet. Regarding plant height, higher correlations, with R^2 of up to 0.55, can be seen at C-band compared to R^2 not higher than 0.36 at L-band.

Looking at the scene-based analysis of airborne data, the correlation between backscattering signals and NDRE is highest at L-band for potato with R^2 = 0.64, while at C-band it is highest for wheat and barley with both R^2 = 0.74. A negative correlation between backscattering signal and NDRE can be observed for both wheat and barley at C-band, which is also partially present in the space-borne correlations. In this regard, both air- and space-borne SAR observations show the attenuation effect on the backscattering signal within crops in co- and cross polarizations, as observed in previous studies [9] (figure 4). Regarding the effect of interception water, L-band tends to be more affected with a mean difference between irrigated and non-irrigated areas of 3.27 dB in the cross-polarized and 2.20 dB in the co-polarized channel. Moreover, the C-band data is influenced less with 1.98 dB in the cross-polarized and 1.78 dB in the co-polarized channel.

6. CONCLUSION

With the SARSense campaign, an extensive multi-frequency SAR time-series dataset was established. Due to the large variety of crops and the large number of high temporal and spatial resolution measurements of various soil and plant parameters, we provide a comprehensive database for SAR-based research on agricultural sites for a variety of crop types. Even though no absolute comparability between air- and space-borne SAR data is possible, the dataset provides insights into both, small-scale and short-term correlations (e.g., interception) as well as more general dynamics and trends of C- and L-band backscatter to soil and plant parameters.

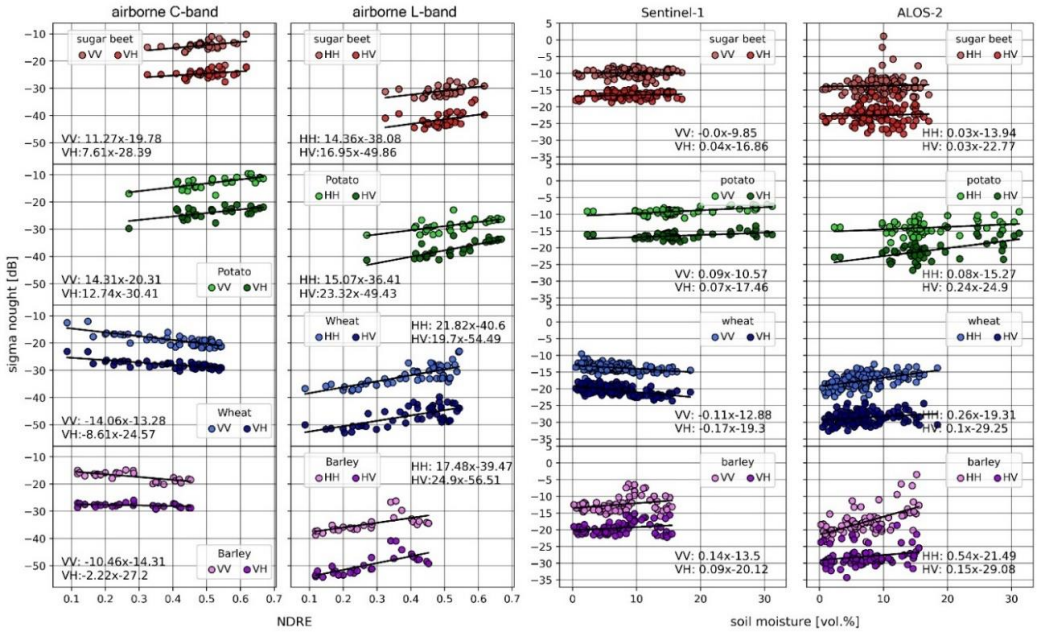

Figure 4 Scatter plots between Normalized Difference Red Edge Index (NDRE) (left) and in situ-based volumetric soil moisture (right) and backscattering signal from co- and cross-polarized channels of C- and L-band air- and space-borne SAR data for four different crop types (sugar beet, potato, wheat and barley).

7. ACKNOWLEDGEMENTS

We gratefully acknowledge funding by the European Space Agency (ESA) under Contract No. 4000125444/18/NL/LF and by the German Ministry of Economic Affairs and Energy (BMWi) through the German Aerospace Center for the AssimEO project (50EE1914A/B). Special thanks go to European Copernicus Satellite Program for providing free access to Sentinel-1 SAR data; the European Space Agency (ESA) and Japan Aerospace Exploration Agency (JAXA) for the ALOS-2 SAR data; MetaSensing for providing the airborne SAR recordings and the FLEXSense campaign (ESA Contract No. 4000125402/18/NL/NA)

8. LITERATURE

[1] Sheffield, J.; Wood, E.F.; Pan, M.; Beck, H.; Coccia, G.; Serrat-Capdevila, A.; Verbist, K. Satellite Remote Sensing for Water Resources Management: Potential for Supporting Sustainable Development in Data-Poor Regions. Water Resour. Res. **2018**, 54, 9724–9758, doi:10.1029/2017WR022437.

[2] Tang, Q.; Gao, H.; Lu, H.; Lettenmaier, D.P. Remote sensing: hydrology. Progress in Physical Geography: Earth and Environment **2009**, 33, 490–509, doi:10.1177/0309133309346650.

[3] Balenzano, A.; Mattia, F.; Satalino, G.; Davidson, M.W.J. Dense Temporal Series of C- and L-band SAR Data for Soil Moisture Retrieval Over Agricultural Crops. IEEE J. Sel. Top. Appl. Earth Observations Remote Sensing **2011**, 4, 439–450, doi:10.1109/JSTARS.2010.2052916.

[4] Bogena, H.R.; Montzka, C.; Huisman, J.A.; Graf, A.; Schmidt, M.; Stockinger, M.; Hebel, C. von; Hendricks-Franssen, H.J.; van der Kruk, J.; Tappe, W.; et al. The TERENO-Rur Hydrological Observatory: A Multiscale Multi-Compartment Research Platform for the Advancement of Hydrological Science. Vadose Zone Journal **2018**, 17, 180055, doi:10.2136/vzj2018.03.0055.

[5] Brogi, C.; Huisman, J.A.; Pätzold, S.; Hebel, C. von; Weihermüller, L.; Kaufmann, M.S.; van der Kruk, J.; Vereecken, H. Large-scale soil mapping using multi-configuration EMI and supervised image classification. Geoderma **2019**, 335, 133–148, doi:10.1016/j.geoderma.2018.08.001.

[6] Rudolph, S.; van der Kruk, J.; Hebel, C. von; Ali, M.; Herbst, M.; Montzka, C.; Pätzold, S.; Robinson, D.A.; Vereecken, H.; Weihermüller, L. Linking satellite derived LAI patterns with subsoil heterogeneity using large-scale ground-based electromagnetic induction measurements. Geoderma **2015**, 241-242, 262–271, doi:10.1016/j.geoderma.2014.11.015.

[7] Brogi, C.; Huisman, J.A.; Herbst, M.; Weihermüller, L.; Klosterhalfen, A.; Montzka, C.; Reichenau, T.G.; Vereecken, H. Simulation of spatial variability in crop leaf area index and yield using agroecosystem modeling and geophysics-based quantitative soil information. Vadose zone j. **2020**, 19, 2026, doi:10.1002/vzj2.20009.

[8] Weihermüller, L.; Huisman, J.A.; Lambot, S.; Herbst, M.; Vereecken, H. Mapping the spatial variation of soil water content at the field scale with different ground penetrating radar techniques. Journal of Hydrology **2007**, 340, 205–216, doi:10.1016/j.jhydrol.2007.04.013.

[9] Wegmüller, U.; Santoro, M.; Mattia, F.; Balenzano, A.; Satalino, G.; Marzahn, P.; Fischer, G.; Ludwig, R.; Floury, N. Progress in the understanding of narrow directional microwave scattering of agricultural fields. Remote Sensing of Environment **2011**, 115, 2423–2433, doi:10.1016/j.rse.2011.04.026.